

Article

RETRACTED: Exploration of Growth Window for Phase-Pure Cubic Boron Nitride Films Prepared in a Pure N₂ Plasma

Wei Gao, Yujing Li, Yuyuan Zhang and Hong Yin *

State Key Laboratory of Superhard Materials, Jilin University, Changchun 130012, China; gwei@jlu.edu.cn (W.G.); yjli16@mails.jlu.edu.cn (Y.L.); yyzhang16@mails.jlu.edu.cn (Y.Z.)

* Correspondence: hyin@jlu.edu.cn

Received: 22 December 2017; Accepted: 23 February 2018; Published: 24 February 2018

Abstract: Cubic boron nitride (c-BN) films were prepared via radio frequency (RF) magnetron sputtering from a hexagonal boron nitride (h-BN) target in a pure N₂ plasma. The composition and microstructure morphology of the BN films with different deposition times under pure N₂ plasma or mixed Ar/N₂ plasma were investigated with respect to the nucleation and growth processes. The pure-phase c-BN growth window was obtained using pure N₂ gas. The effects of pure N₂ gas on the growth mechanism, structural morphology, and internal compressive stress of the as-synthesized c-BN films were studied. Using pure N₂ gas instead of additional Ar resulted in improved microstructure quality and much reduced compressive stress, suggesting a fundamental strategy for achieving high-quality c-BN films.

Keywords: cubic boron nitride; magnetron sputtering; gas composition; nucleation; substrate bias

1. Introduction

Cubic boron nitride (c-BN), an analog of diamond, exhibits many outstanding properties, such as extreme hardness, wide band gap, negative electron affinity, and high thermal conductivity. Furthermore, c-BN also has numerous properties, such as higher chemical stability, both p- and n-type doping availability, surface smoothness, biocompatibility, and hydrophilicity, that make it superior to diamond for applications in protection coatings and cutting tools, high-temperature electronics, ultraviolet (UV) detectors, deep-UV light-emitting diodes, and bio-/chemi-sensors [1,2]. However, synthesizing device-quality large-area single crystals of c-BN has not been established despite considerable progress [3–5] and single crystal wafers are not available yet.

So far, various techniques have been employed to grow c-BN films, including physical vapor deposition [3,6] and plasma-enhanced chemical vapor deposition [7,8]. The energetic plasma surface process is essential for the nucleation and growth of c-BN thin films regardless of growth technique. The chemical routes usually use deleterious and corrosive gases, such as H, C, Na, F, Ar, and He, unavoidably leaving contaminants in c-BN films. The uncontrolled presence of impurities involved in the growth process leads to uncertainty of the electronic transport mechanism in intrinsic samples, which is mirrored by the fact that numerous luminescence centers have been observed in c-BN crystals prepared by high-pressure, high-temperature synthesis, and for many of those it is not clear whether they can be attributed to an intrinsic defect or to a precursor impurity [9–12]. On the other hand, most physical vapor deposition methods rely on either energetic ion bombardment with the substrate being negatively biased or electron assistance with the substrate being positively biased, which is generally assisted by massive ions of Ar [13,14]. Such involvement of Ar ions may cause resputter of the deposited film, structural damage, and stress accumulation, especially under high ion energy conditions [15,16]. Although introducing H₂ into the working gases can effectively etch the *sp*² phase,

leaving an sp^3 phase [17], the assistance of Ar for energetic ion bombardment is the major reason for the poor adhesion that is usually found, which severely hinders the application of c-BN films.

Hofsass et al. [18] attempted to grow c-BN film by using only $11B^+$ and $14N^+$ ions on heated Si substrates in ultra-high vacuum (UHV) environment using mass separated ion beam deposition. For the first time, no additional ions, such as Ar^+ , were involved in the growth process. Litvinov et al. [19] obtained thick c-BN films with reduced bias voltage in pure nitrogen gas using an electron cyclotron resonance source. Later, Yap et al. [20] investigated c-BN films using plasma-assisted pulsed-laser deposition in pure N_2 radio frequency (RF) plasma. They found that all c-BN films prepared in pure N_2 plasma were significantly improved in stability versus those prepared in Ar-rich plasma. These approaches, however, normally require a complex apparatus and are energy consuming. Thus, it is critical to find a simple and effective way to synthesize high-quality c-BN films by using growth species such as B^+ and N^+ ions exclusively.

Diamond has been reported as a perfect nucleation surface for epitaxial growth of c-BN due to the small lattice mismatch of these two materials [3,4,21,22]. Epitaxy of c-BN/diamond is attracting significant attention for both basic crystal engineering and optoelectronic applications. From this point of view, imitating nucleation of c-BN on diamond surface is very interesting, as well as the growth of high-quality c-BN films. As has been demonstrated previously [23], the deposition of a thin h-BN interfacial layer followed by an intended c-BN film can provide a pure c-BN polycrystalline top layer as a nucleation template for subsequent growth. Generally, elevated substrate temperatures combined with significantly enhanced ion bombardment are needed in order to obtain the pure cubic phase at the growth layer. Here, we report on the deposition of high-quality c-BN films on Si substrates by the conventional RF magnetron sputter method without additional argon ion bombardment. An important aspect previously overlooked in the deposition process of c-BN film is optimization of the experimental parameters using pure N_2 gas in nucleation and growth. We therefore focus on characterization of the c-BN films prepared using pure N_2 or mixed Ar/ N_2 plasma with different deposition times, which enables investigation of the difference between these two parameters in the initial nucleation stage of the films. The pure-phase c-BN growth window is obtained when using pure N_2 gas. Furthermore, using pure N_2 gas instead of additional Ar results in improved microstructure quality and much reduced compressive stress, suggesting a fundamental strategy for achieving high-quality c-BN films.

2. Experiments

2.1. Deposition

c-BN films were deposited on silicon (100) substrates using the RF magnetron sputtering method. All silicon wafers underwent ultrasonic pretreatment in a petroleum ether solution for 3 min, then were washed by deionized (DI) H_2O . Second, the silicon wafers were immersed in a boiled solution of $NH_4 \cdot OH$, H_2O_2 , and DI H_2O (1:2:5) for 2 min, then washed with DI H_2O to remove the organic contaminants. Later, the silicon wafers were immersed in a solution of HCl, H_2O_2 , and DI H_2O (1:2:8) for 2 min at room temperature, then washed with DI H_2O , to remove the inorganic contaminants. Before being mounted in the deposition chamber, the wafers were immersed in a diluted 100% HF solution and rinsed with DI H_2O to remove the native SiO_2 , and finally blown dry with nitrogen gas. The base pressure was maintained below 5×10^{-4} Pa. A hexagonal BN target (pure 99.9%, 3 mm thick, 50 mm in diameter) was mounted on a water-cooled magnetron gun, which was coupled on an RF (13.56 MHz) generator via a matching network (SKY, Chinese Academy of Sciences (CAS), Shenyang, China). The substrate holder was 40 mm from the target. The target was sputter-cleaned for 5 min before each deposition. The RF power applied to the target was 80 W in the present work. In order to study the nucleation and growth stage, the films were prepared in two groups. In the first group of experiments, c-BN films were deposited under -250 V substrate bias voltage at 470 °C for different deposition times to investigate the influence of using pure N_2 and 1:1 Ar/ N_2 in the initial

nucleation stage. In the second group, the c-BN films were deposited at 800 °C for 40 min on top of a template c-BN layer to explore the growth window of pure c-BN films using pure N₂ and 1:1 Ar/N₂. The template c-BN layers were prepared in pure N₂ plasma under −250 V substrate bias voltage at 470 °C for 30 min. The phase purity and structure of the films were analyzed.

2.2. Characterization

Fourier transform infrared spectroscopy (FTIR; Nicolet Avatar 370, Thermo Fisher Scientific, Waltham, MA, USA) was used to provide information about phase composition and film stress in transmission modes in the 400–4000 cm^{−1} range. The chemical states on the surfaces of the deposited films were studied by monochromic X-ray photoelectron spectrometry (XPS; PREVAC XPS/UPS system with Al K α radiation, PreVac, Rogów, Poland). The surface morphology of the films was investigated by atomic force microscopy (AFM; Digital Instruments Multimode AFM, Bruker, Karlsruhe, Germany) and scanning electron microscopy (SEM; Quanta Magellan 400, Thermo Fisher Scientific, Waltham, MA, USA) equipped with electron beam, working at 10 kV.

3. Results and Discussion

Figure 1a shows the FTIR spectra obtained from BN films using pure N₂ plasma at 470 °C with different deposition times. The absorption band at 1091 cm^{−1} is due to the transverse optical (TO) mode of c-BN, while two absorption bands at 1400 and 770 cm^{−1} correspond to the h-BN phase and result from the in-plane B–N stretching mode and the out-of-plane B–N–B bending vibration, respectively [17]. It can be clearly observed that there is a continuous increase of the intensity of c-BN peak, while the positions of the c-BN peaks have no obvious shift with increased deposition time. The intensity of the h-BN absorption peaks exhibits no obvious change. The IR absorption spectra of BN films using 1:1 Ar/N₂ plasma at different deposition times are displayed in Figure 1b. In this case, the absorption bands of all c-BN films stay at 1100 cm^{−1}. With increased deposition time, the intensity of c-BN peak also increases, whereas no obvious shift is observed for its position. Compared to the film grown using pure N₂, it is noticeable that at the deposition time of 10 min, the film grown using Ar/N₂ already exhibits trivial cubic phases, which suggests that involvement of Ar during the film deposition causes the cubic phase to nucleate faster than the one using pure N₂. The cubic volume fraction can be estimated directly from relative intensities of the c-BN TO peak (I_{c-BN}) and the h-BN peak at 1400 cm^{−1} (I_{h-BN}):

$$Q_{c-BN} = \frac{I_{c-BN}}{I_{c-BN} + I_{h-BN}} \quad (1)$$

Thus, we can estimate the cubic volume fraction of each film, which is 47%, 60%, and 70% for the film using pure N₂ and 50%, 71%, and 80% for the film using Ar/N₂. The cubic phase content in the c-BN films using Ar/N₂ plasma is higher than that using pure N₂ plasma at the same deposition time, since the increased bombardment of the c-BN films by energetic Ar ions induces a higher growth rate. The thickness of the film prepared using Ar/N₂ for 40 min is about 50 nm, corresponding to a growth rate of 1.25 nm/min, while the growth rate of the film prepared using pure N₂ is slightly lower (~1.12 nm/min).

In addition, the positions of c-BN TO mode peaks shift toward the lower wavenumber direction for the films grown in pure N₂ plasma compared to those using mixed Ar/N₂ plasma. The compressive stress for the film can be estimated from

$$\sigma = \frac{\omega_C - 1065 \text{ cm}^{-1}}{5 \text{ GPa/cm}^{-1}} \quad (2)$$

This strongly indicates reduced compressive stress in the c-BN film without additional argon ion bombardment [24]. Both c-BN films grown, regardless of additional Ar ion bombardment, reveal the well-known layered structure of amorphous/hexagonal/cubic phases, which are confirmed by the following surface characterizations. The thickness of the initial layer of hexagonal structure estimated

from the sp^2 absorbance and an absorbance coefficient (h-BN: $25,000 \text{ cm}^{-1}$) was approximately 15 nm for the film grown using pure N_2 plasma and 10 nm for the film grown using Ar/N_2 plasma [25]. It has also been observed that an increase in the N_2 plasma concentration extends the thickness of the interlayer [26].

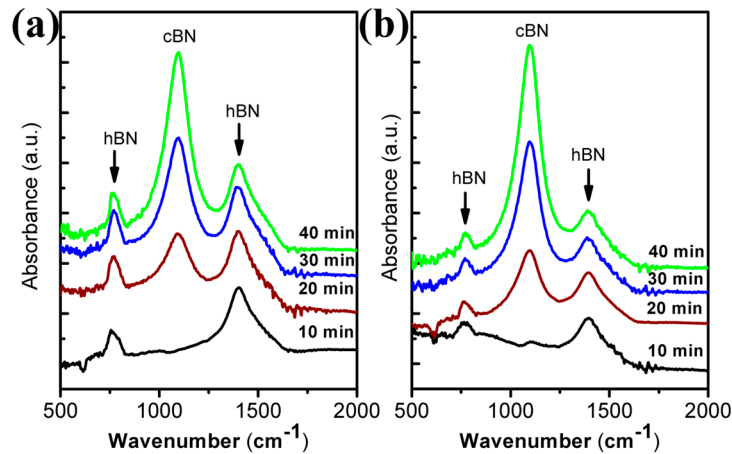


Figure 1. FTIR spectra for cubic boron nitride (c-BN) films grown at different times under (a) pure N_2 plasma and (b) $\text{Ar}:\text{N}_2 = 1:1$ plasma. The c-BN transverse optical (TO) peak stays at 1091 and 1100 cm^{-1} in the two-gas system.

It is well known that fluctuations in the near surface atomic structure of the studied films will lead to variations in the density and, consequently, the plasmon energies. Energy loss function delivers more information on the influence of the near surface structure. Figure 2a,b shows energy loss spectra based on $\text{N}1s$ core level electron excitations of the BN films using pure N_2 plasma and Ar/N_2 plasma with different deposition times. For the films grown with deposition time from 10 to 40 min, minor variations are detected from the bottom to the top curve as far as the plasmon energy and the general shape of the loss function are concerned. A prominent peak can be observed at 8 eV in films grown using either pure N_2 or Ar/N_2 with a deposition time of 10 min. In the BN system, the peak at 8 eV is due to a $\pi-\pi^*$ interband transition [27], which can only occur in h-BN, thus acts as a fingerprint for h-BN. The peak located at about 27 eV is attributed to the volume plasmon of h-BN as well. This indicates that the surface of the films is composed mainly of the h-BN phase at the initial nucleation stage. With longer deposition time, differences in the h-BN and c-BN loss functions are visible as increased plasmon energy in the cubic phase reflecting the higher density, accompanied by the absence of $\pi-\pi^*$ related features, attenuation of the volume plasmon of h-BN, and the appearance of additional structures at energies higher than 30 eV [28,29]. These results unambiguously reflect the layered structure of amorphous/hexagonal/cubic phases. Another important detail of the loss spectrum for the BN film grown using pure N_2 gas for 10 min is that the small peak at about 4.6 eV is due to the N–N bonds [30], which is invisible for the film grown using Ar/N_2 . This strongly suggests the existence of N–N configurations in hexagonal BN layer supplied by pure N_2 bombardment at the initial stage.

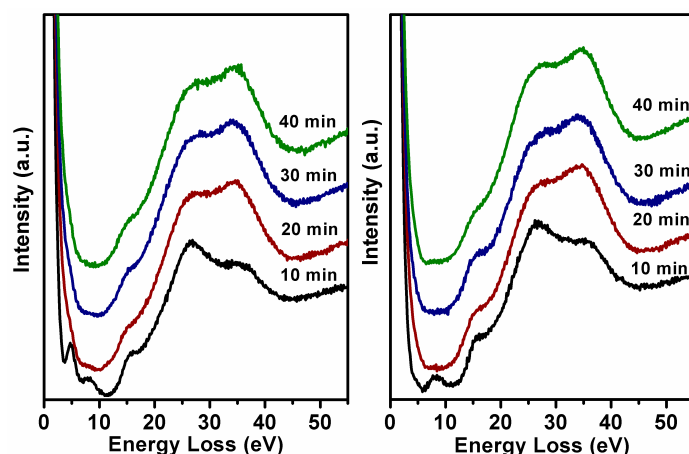


Figure 2. Energy loss function based on N 1s plasmon for c-BN film deposition times using (a) pure N₂ plasma and (b) mixed Ar/N₂ plasma.

To gain further insight into the differences in the nucleation process of c-BN films using pure N₂ plasma and mixed Ar/N₂ plasma, a nucleation sequence was studied in detail by means of AFM measurements. Figure 3 presents root mean squared (RMS) roughness as a function of deposition time. Typical AFM images recorded as surface morphology for these films are shown in Figure S5. Several AFM images were taken at different positions for each film surface for the RMS estimation. Thus it was expected that the errors involved were random and could be cancelled out when statistical results were averaged. After 10 min of growth, the RMS roughness of the films was estimated as 0.74 ± 0.04 nm and 1.20 ± 0.07 nm for pure N₂ plasma and mixed Ar/N₂ plasma, respectively. It is known from FTIR measurements and energy loss functions that the film for pure N₂ growth consists mainly of h-BN after 10 min; however, the cubic phase already starts to nucleate for the film grown with Ar/N₂. It was previously reported that bombardment of Ar ions can penetrate into the growing h-BN film during deposition and induce accumulation of compressive stress, consequently influencing the microstructure of the h-BN layer [31]. As a result, the initial h-BN layer becomes rougher, since a randomly oriented laminate structure forms under the ion bombardment. Such bombardment leads to high enough compressive stresses to favor c-BN thermodynamically. It is believed that the higher roughness of h-BN film grown with argon ion bombardment is caused by Ar⁺ ion penetration into the film during deposition. In order to confirm this speculation, the XPS spectra of survey and Ar 2*p* core level (Figure 4) for the BN films deposited for 10 min were measured. This clearly shows that the Ar ions reside in the BN film prepared in Ar/N₂ plasma. However, there is no contaminant of Ar in h-BN film grown without Ar ion bombardment. It has been reported that residual stress of h-BN is reduced after annealing at high temperature, which also explains how the buried Ar atoms could diffuse out during annealing [24].

As the deposition time increases more than 10 min and the subsequent cubic structure accumulates continuously, the surface of the c-BN films prepared in Ar/N₂ plasma becomes very smooth. The RMS roughness of these films with deposition times of 20, 30, and 40 min was 0.81 ± 0.06 nm, 0.68 ± 0.04 nm, and 0.79 ± 0.05 nm, respectively. Contrarily, the RMS roughness of the pure N₂ prepared films with deposition times of 20, 30, and 40 min was estimated as 2.23 ± 0.10 nm, 2.75 ± 0.11 nm, and 1.26 ± 0.11 nm, respectively. Thus, the films prepared without argon ion bombardment were much rougher. After 40 min, the surface became smooth again. This was probably due to the fine crystallites of c-BN films with mixed Ar/N₂ plasma, considering higher energetic ion bombardment with the assistance of Ar during film growth. Furthermore, Ar ion bombardment has been found to prevent the growth of larger crystallites [32]. Therefore, the film surface obtained was composed of fine crystallites of several to tens of nanometers in size. Nevertheless, both systems of the c-BN films showed rather smooth surface over a large area regardless of Ar (see Supplementary Materials). The results of

roughness estimation indicate that moderate ion bombardment without the use of Ar ions is expected to improve the crystalline quality.

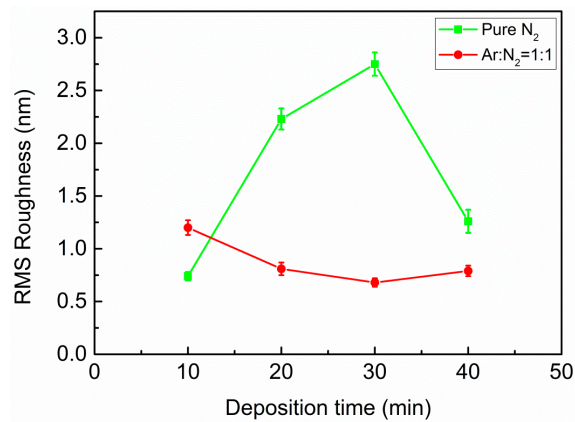


Figure 3. Root mean squared (RMS) roughness as a function of deposition time for c-BN films grown using pure N₂ plasma (square) and Ar/N₂ plasma (circle). The corresponding atomic force microscopy (AFM) images (4 μm × 4 μm) representing each data point are displayed in the Supplementary Materials.

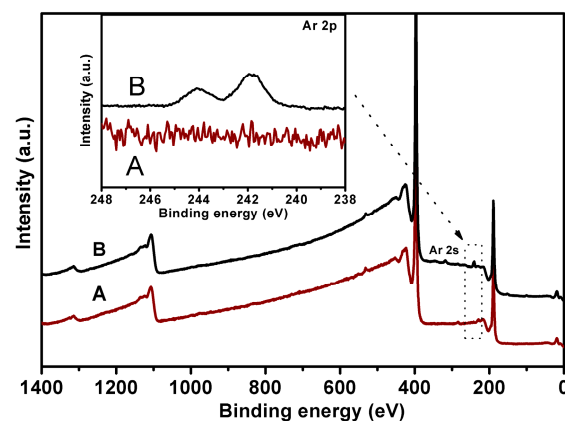


Figure 4. X-ray photoelectron spectrometry (XPS) survey spectra for c-BN films with (A) pure plasma and (B) mixed Ar/N₂ plasma after 10 min deposition. The inset shows Ar 2p core level spectra for the c-BN films.

To further study the differences in growth conditions using pure N₂ and Ar/N₂ plasma, we focused on the c-BN layers grown on c-BN template nucleate layer in a two-step manner, in which the top layer of c-BN was expected to provide pure growth information. In the first step, template c-BN films were prepared in pure N₂ plasma under −250 V substrate bias voltage at 470 °C for 30 min. The template c-BN film has been characterized as shown in the Supplementary Materials. In the second step, the substrate temperature was increased up to 800 °C and depositions were performed for 40 min at substrate bias voltages of −125, −150, −200, −250, and −275 V. Figure 5a,b show a series of FTIR absorption spectra of the second BN films at different bias voltages with pure N₂ plasma and Ar/N. The relative height of IR peak is related to the thickness of the film under investigation. For the bias voltage in this range, further growth of the film was observed. The thickness of the film grown at −150 V for both gas compositions was roughly measured to be 50 nm by Taly step. It can be observed that the growth rate at −150 V was higher than that at the other bias voltages. When the bias voltage was changed from −150 to −275 V, the etching rate was enhanced as well, resulting in a monotonously

reduced growth rate. No further growth of films occurred after the second growth when the bias voltage was beyond -300 V, implying that the resputtering regime was reached.

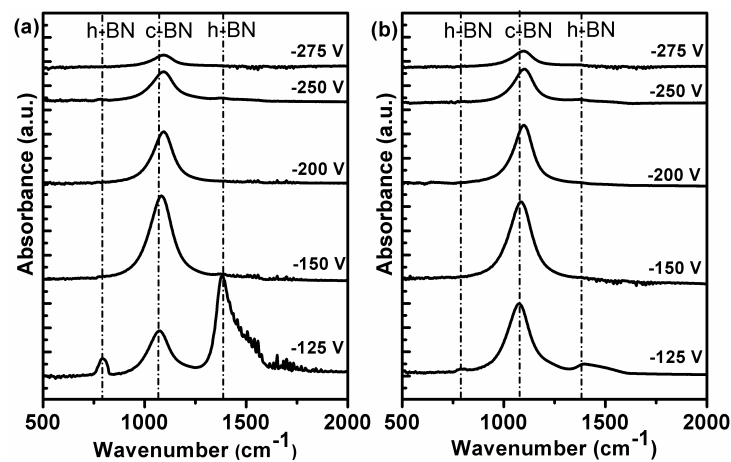


Figure 5. FTIR spectra of a series of c-BN films deposited at various substrate biases from -125 to -275 V with (a) pure N_2 and (b) $Ar:N_2 = 1:1$ in the working gas after the second step.

In addition, the critical bias voltage was explored and compared when using pure N_2 and Ar/N_2 plasma. This critical value is considered to be necessary for incubation of c-BN nucleation. For the films at bias voltages of -150 , -200 , -250 , and -275 V, it is clear that the FTIR spectra are dominated by only one peak, which is characteristic for the TO mode of the cubic phase. The absence of characteristic h-BN peaks strongly indicates 100% cubic phase without any h-BN. On the other hand, the cubic content of c-BN film at bias voltage of -125 V with Ar/N_2 plasma was estimated to be 87%, significantly higher than that with pure N_2 (30% of cubic phase after second growth). This shows the critical bias voltage for growth of the pure cubic phase of BN films and the dependence of the critical voltage on the working gas. Deposition of pure c-BN films using Ar/N_2 was obtained at lower bias voltage than when using pure N_2 gas in the present experiments. Nevertheless, in both cases, the pure cubic phase of BN films was obtained within the bias voltage window from -150 to -275 V.

Besides, one may notice that for both cases, c-BN TO peaks in the FTIR spectra shift toward lower frequencies with reduced bias voltage during growth. This shift is consistent with the reduced compressive stress in the films grown at lower bias [33]. In order to better compare the differences, the c-BN TO peak positions of the pure cubic phase films at bias voltages of -150 , -200 , -250 , and -275 V displayed in Figure 5 were plotted as a function of substrate bias voltage in Figure 6. For both working gas systems, the c-BN TO peak slightly shifts toward higher frequencies at the bias voltage of -250 V and further shifts toward lower frequencies gradually. Since only phase-pure cubic BN films were compared in the present case, the subsequent shifting of the c-BN peak position as bias voltage decreased is predominantly residual compressive stress due to ion bombardment because of their comparative film thickness. Another important aspect is that the c-BN TO peak frequencies of the films grown using pure N_2 ion bombardment were rather low compared with those of c-BN films grown using Ar/N_2 plasma at the same bias voltage, indicating lower residual compressive stress. This was confirmed by the observation that the high cubic content containing BN films using Ar as reactive gas often delaminated in air, whereas those using pure N_2 gas were much more stable after several months in air. This suggests that the moderate ion bombardment using pure N_2 gas is propitious to grow less stressed c-BN films, favoring the growth of highly stable and robust pure c-BN films.

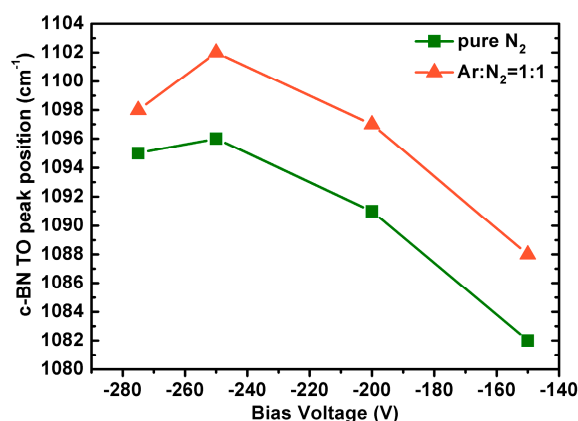


Figure 6. c-BN TO peak position vs. substrate bias voltage. For unambiguous understanding, all these films are 100% cubic.

4. Conclusions

In conclusion, we have demonstrated that high-quality c-BN films can be grown on silicon wafers by the RF magnetron sputtering method with pure N₂ as working gas. A comprehensive study of c-BN films prepared with pure N₂ or mixed Ar/N₂ plasma for nucleation and further growth was systematically carried out by FTIR, XPS, and AFM. The incubated Ar in the interfacial h-BN layer grown with Ar/N₂ gas led to a randomly oriented structure, and therefore built up compressive stress, which could be improved by exclusively using pure N₂ as sputtering and reactive gas. A two-step process was utilized to investigate the nucleation and growth of c-BN separately. A growth window of substrate bias voltage for c-BN growth after nucleation was obtained. When the bias voltage was higher than the upper limit, the film was etched away, and when it was lower than the lower limit, the cubic phase did not nucleate. Despite the relatively narrower growth window of predominantly cubic content BN films as a function of substrate bias voltage when using pure N₂ ion bombardment than that using pure N₂ plasma, it was possible to obtain pure cubic phase of BN films at certain voltage values. Although the current study is based on nucleation of c-BN on silicon substrate by using only growth species B and N, it opens up a pathway toward understanding the fundamental nucleation of c-BN and future epitaxial growth of c-BN on an appropriate substrate with small lattice mismatch, e.g., diamond single crystal and CVD diamond films using the magnetron sputtering method. Furthermore, using pure N₂ gas during the growth process will rule out the possibility of Ar or other precursor impurities residing in the film, and consequently improve the film's purity and quality with little damage from ion bombardment.

Supplementary Materials: The following are available online at www.mdpi.com/2079-6412/8/2/82/s1. Figure S1: Typical SEM images of c-BN films grown using (a,b) Ar/N₂ and (c,d) pure N₂; Figure S2: Typical confocal microscopy image of c-BN film grown using pure N₂; Figure S3: Typical Taly step profilographs of different positions (a–c) on a 200 nm thick c-BN film grown using pure N₂; Figure S4: Typical SEM image of c-BN film grown using pure N₂; Figure S5: Typical AFM images of c-BN films grown using (a–d) pure N₂ plasma and (e–h) Ar/N₂ plasma: (a,e), (b,f), (c,g), and (d,h) for the c-BN films with deposition times of 10, 20, 30, and 40 min, respectively; Figure S6: FTIR spectrum of a typical c-BN template film used in the present work; Figure S7: (a) XPS survey spectrum and core level spectra of (b) B 1s and (c) N 1s of a typical c-BN template film used in the present work; Figure S8: (a) AFM and (b) SEM images of a typical c-BN template film used in the present work.

Acknowledgments: Financial support from the National Natural Science Foundation of China (Grant Nos. 51572105 and 61504046) is especially acknowledged. Hong Yin is grateful to the Scientific Research Foundation for the Returned Overseas Chinese Scholars, State Education Ministry. Financial support from the development and reform commission of Jilin Province (Grant No. 2015Y050) and the scientific research foundation for the returned overseas of Jilin Province is also appreciated.

Author Contributions: Hong Yin and Wei Gao conceived and designed the experiments; Wei Gao performed the experiments; Hong Yin and Wei Gao analyzed the data; Yujing Li and Yuyuan Zhang contributed reagents/materials/analysis tools; Hong Yin wrote the paper.

Conflicts of Interest: The authors declare no conflict of interest.

References

1. Teii, K.; Matsumoto, S.; Robertson, J. Electron field emission from nanostructured cubic boron nitride islands. *Appl. Phys. Lett.* **2008**, *92*, 013115. [[CrossRef](#)]
2. Zhang, X.W. Doping and electrical properties of cubic boron nitride thin films: A critical review. *Thin Solid Films* **2013**, *544*, 2–12. [[CrossRef](#)]
3. Zhang, X.W.; Boyen, H.G.; Deyneka, N.; Ziemann, P.; Banhart, F.; Schreck, M. Epitaxy of cubic boron nitride on (001)-oriented diamond. *Nat. Mater.* **2003**, *2*, 312–315. [[CrossRef](#)] [[PubMed](#)]
4. Zhang, W.; Bello, I.; Lifshitz, Y.; Chan, K.M.; Meng, X.; Wu, Y.; Chan, C.Y.; Lee, S.-T. Epitaxy on diamond by chemical vapor deposition: A route to high-quality cubic boron nitride for electronic applications. *Adv. Mater.* **2004**, *16*, 1045–1408. [[CrossRef](#)]
5. Hirama, K.; Taniyasu, Y.; Karimoto, S.I.; Krockenberger, Y.; Yamamoto, H. Single-crystal cubic boron nitride thin films grown by ion-beam-assisted molecular beam epitaxy. *Appl. Phys. Lett.* **2014**, *104*, 092113. [[CrossRef](#)]
6. Le, Y.K.; Oechsner, H. On the influence of substrate temperature for cubic boron nitride growth. *Thin Solid Films* **2003**, *437*, 83–88. [[CrossRef](#)]
7. Bello, I.; Chong, Y.M.; Leung, K.M.; Chan, C.Y.; Ma, K.L.; Zhang, W.J.; Lee, S.T.; Layyous, A. Cubic boron nitride films for industrial applications. *Diam. Relat. Mater.* **2005**, *14*, 1784–1790. [[CrossRef](#)]
8. Huang, P.C.; Wong, M.S. Nanostructures of mixed-phase boron nitride via biased microwave plasma-assisted CVD. *Vacuum* **2014**, *100*, 66–70. [[CrossRef](#)]
9. Yin, H.; Boyen, H.G.; Ziemann, P.; Dohuard, B.; Houssiau, L.; Renaux, F.; Hecq, M.; Bittencourt, C. Purity of epitaxial cubic boron nitride films on (001) diamond—A prerequisite for their doping. *Diam. Relat. Mater.* **2008**, *17*, 276–282. [[CrossRef](#)]
10. Zhang, W.J.; Kanda, H.; Matsumoto, S. Cathodoluminescence of cubic boron nitride films deposited by chemical vapor deposition. *Appl. Phys. Lett.* **2002**, *81*, 3356. [[CrossRef](#)]
11. Manfredotti, C.; Giudice, A.L.; Paolini, C.; Vittone, E.; Fizzotti, F.; Cossio, R. Characterization of impurities in cubic boron nitride crystallites with thermoluminescence and ionoluminescence. *Phys. Stat. Sol. (a)* **2004**, *201*, 2566–2572. [[CrossRef](#)]
12. Taniguchi, T.; Teraji, T.; Koizumi, S.; Watanabe, K.; Yamaoka, S. Appearance of n-type semiconducting properties of cBN single crystals grown at high pressure. *Jpn. J. Appl. Phys.* **2002**, *41*, L109. [[CrossRef](#)]
13. Deyneka, N.; Zhang, X.W.; Boyen, H.G.; Ziemann, P.; Fukarek, W.; Kruse, O.; Moller, W. Depth profiles of Argon incorporated into Boron Nitride films during preparation and their temperature dependent evolution. *Diam. Relat. Mater.* **2003**, *12*, 37–46. [[CrossRef](#)]
14. Tzeng, Y.; Zhu, H. Electron-assisted deposition of cubic boron nitride by r.f. magnetron sputtering. *Diam. Relat. Mater.* **1999**, *8*, 1402–1405. [[CrossRef](#)]
15. McKenzie, D.R.; McFall, W.D.; Sainy, W.G.; Davis, C.A.; Collins, R.E. Compressive stress-induced formation of cubic boron-nitride. *Diam. Relat. Mater.* **1993**, *2*, 970–976. [[CrossRef](#)]
16. Li, B.S.; Wang, T.G.; Ding, J.C.; Cai, Y.J.; Shi, J.; Zhang, X.T. Influence of N₂/Ar flow ratio on microstructure and properties of the AlCrSiN coatings deposited by high-power impulse magnetron sputtering. *Coatings* **2018**, *8*, 3. [[CrossRef](#)]
17. Zhao, Y.; Gao, W.; Xu, B.; Li, Y.-A.; Li, H.-D.; Gu, G.-R.; Yin, H. Thick c-BN films deposited by radio frequency magnetron sputtering in argon/nitrogen gas mixture with additional hydrogen gas. *Chin. Phys. B* **2016**, *25*, 106801. [[CrossRef](#)]
18. Hofsass, H.; Ronning, C.; Griesmeier, U.; Gross, M.; Reinke, S.; Kuhr, M. Cubic boron-nitride films grown by low-energy B⁺ and N⁺ ion-beam deposition. *Appl. Phys. Lett.* **1995**, *67*, 46–48. [[CrossRef](#)]
19. Litvinov, D.; Clarke, R. Reduced bias growth of pure-phase cubic boron nitride. *Appl. Phys. Lett.* **1997**, *71*, 1969–1971. [[CrossRef](#)]
20. Yap, Y.K.; Aoyama, T.; Kida, S.; Mori, Y.; Sasaki, T. Synthesis of adhesive c-BN films in pure nitrogen radio-frequency plasma. *Diam. Relat. Mater.* **1999**, *8*, 382–385. [[CrossRef](#)]
21. Shammas, J.; Yang, Y.; Wang, X.; Koeck, F.A.M.; McCartney, M.R.; Smith, D.J.; Nemanich, R.J. Band offsets of epitaxial cubic boron nitride deposited on polycrystalline diamond via plasma-enhanced chemical vapor deposition. *Appl. Phys. Lett.* **2017**, *111*, 171604. [[CrossRef](#)]

22. Chen, C.L.; Wang, Z.C.; Kato, T.; Shibata, N.; Taniguchi, T.; Ikuhara, Y. Misfit accommodation mechanism at the heterointerface between diamond and cubic boron nitride. *Nat. Commun.* **2015**, *6*, 6327. [[CrossRef](#)] [[PubMed](#)]
23. Boyen, H.G.; Deyneka, N.; Ziemann, P.; Banhart, F. Ion beam assisted growth of c-BN films on top of c-BN substrates—A HRTEM study. *Diamond Relat. Mater.* **2002**, *11*, 38–42. [[CrossRef](#)]
24. Yang, H.S.; Chen, A.L.; Qiu, F.M. Cubic boron nitride film residual compressive stress relaxation by post annealing. *Diam. Relat. Mater.* **2011**, *20*, 1179–1182. [[CrossRef](#)]
25. Zhang, X.W.; Yin, H.; Boyen, H.G.; Ziemann, P.; Ozawa, M. Effects of crystalline quality on the phase stability of cubic boron nitride thin films under medium-energy ion irradiation. *Diam. Relat. Mater.* **2005**, *14*, 1482–1488. [[CrossRef](#)]
26. Yoshida, T. Vapour phase deposition of cubic boron nitride. *Diam. Relat. Mater.* **1996**, *5*, 501–507. [[CrossRef](#)]
27. Xu, Y.-N.; Ching, W.Y. Calculation of ground-state and optical properties of boron nitrides in the hexagonal, cubic, and wurtzite structures. *Phys. Rev. B* **1991**, *44*, 7787–7798. [[CrossRef](#)]
28. Reinke, P.; Oelhafen, P.; Feldermann, H.; Ronning, C.; Hofsass, H. Hydrogen-plasma etching of ion beam deposited c-BN films: An in situ investigation of the surface with electron spectroscopy. *J. Appl. Phys.* **2000**, *88*, 5597–5604. [[CrossRef](#)]
29. Widmayer, P.; Boyen, H.G.; Ziemann, P.; Reinke, P.; Oelhafen, P. Electron spectroscopy on boron nitride thin films: Comparison of near-surface to bulk electronic properties. *Phys. Rev. B* **1999**, *59*, 5233–5241. [[CrossRef](#)]
30. Gritsenko, V.A.; Morokov, Y.N.; Novikov, Y.N. Electronic structure of amorphous Si₃N₄: Experiment and numerical simulation. *Appl. Surf. Sci.* **1997**, *113*, 417–421. [[CrossRef](#)]
31. Kim, H.S.; Park, J.K.; Baik, Y.J.; Choi, I.H. Origin of residual stress in the formation of boron nitride film by sputtering with Ar ions. *J. Appl. Phys.* **2003**, *94*, 3057–3060. [[CrossRef](#)]
32. Freudenstein, R.; Klett, A.; Kulisch, W. Investigation of the nucleation of c-BN by AFM measurements. *Thin Solid Films* **2001**, *398*, 217–221. [[CrossRef](#)]
33. Bello, I.; Chan, C.Y.; Zhang, W.J.; Chong, Y.M.; Leung, K.M.; Lee, S.T.; Lifshitz, Y. Deposition of thick cubic boron nitride films: The route to practical applications. *Diam. Relat. Mater.* **2005**, *14*, 1154–1162. [[CrossRef](#)]



© 2018 by the authors. Licensee MDPI, Basel, Switzerland. This article is an open access article distributed under the terms and conditions of the Creative Commons Attribution (CC BY) license (<http://creativecommons.org/licenses/by/4.0/>).